Chapter 5
Direct Surface Current Field Imaging from Space by Along-Track InSAR and Conventional SAR

Roland Romeiser, Johnny Johannessen, Bertrand Chapron, Fabrice Collard, Vladimir Kudryavtsev, Hartmut Runge, and Steffen Suchandt

5.1 Introduction

Since the SEASAT mission in 1978 (Fu and Holt, 1982), spaceborne synthetic aperture radars (SARs) have acquired millions of high-resolution images of ocean scenes, which have been used for applications such as wave and wind retrievals, oil pollution monitoring, ship detection, sea ice monitoring, and the interpretation of signatures of surface current gradients over oceanic fronts, internal waves, and shallow-water bathymetry. Unfortunately, despite the fact that a SAR is a Doppler radar, conventional SAR images do not provide direct information on target velocities, since the Doppler information in the raw data is normally utilised to obtain the highest possible spatial resolution in flight (azimuth) direction. In a process called aperture synthesis, targets are mapped to azimuthal locations in the image where their contribution to the spectrum of the received signal during the SAR overpass appears at a Doppler frequency of 0. This implies the assumption that targets have a radial (line-of-sight) velocity of 0. Targets with a nonzero radial velocity will appear shifted in azimuth direction, and it is sometimes possible to retrieve their velocity from the visible displacement (e.g. between train and track or between ship and wake), but this is not possible for distributed targets such as the ocean surface.

Within the last decade, considerable progress has been made in the development of two techniques that do permit a direct retrieval of line-of-sight surface current fields from SAR data. One technique, called along-track interferometry (ATI), requires a second antenna. The other technique is based on Doppler centroid estimates from conventional SAR raw data at a reduced spatial resolution. Both techniques have been demonstrated in several experiments, and they are available for immediate use with existing satellites. The direct imaging of surface currents at relatively high spatial resolutions is particularly attractive for applications for which radar altimetry (e.g. Wunsch and Stammer, 1998) does not work and

R. Romeiser (✉)
Rosenstiel School of Marine and Atmospheric Science, University of Miami, Miami, FL 33149-1031, USA
e-mail: rromeiser@rsmas.miami.edu

V. Barale et al. (eds.), *Oceanography from Space*,
DOI 10.1007/978-90-481-8681-5_5,

ground- or ship-based remote sensing systems (e.g. Palmer, 1991; Essen et al., 2000; Plant et al., 2005) cannot be deployed easily.

5.2 How to Measure Currents by SAR

Although the idea of exploiting Doppler centroid anomalies of conventional SAR raw data for current retrievals was formulated more than 30 years ago (Shuchman, 1979), it did not get much attention until an impressive demonstration with ENVISAT ASAR data was published in 2005 (Chapron et al., 2005). In the meantime, the ATI technique had been proposed by Goldstein and Zebker (1987) and demonstrated in several experiments. Initially, the ATI technique promised current measurements at full SAR resolution, while a Doppler centroid anomaly analysis seemed to reduce the SAR to a coarse-resolution real aperture radar, but as a result of suboptimal system parameters of available spaceborne ATI systems on the one hand and the development of optimised methods for Doppler centroid estimates on the other hand, differences between actual results of the two techniques are much smaller than one might expect. Let us have a brief look at the theoretical background.

5.2.1 Along-Track Interferometry

The ATI technique is based on interferometric combination of two complex SAR images of the same scene, which are acquired with a short time lag on the order of milliseconds. Phase differences between pixels of the two images are proportional to Doppler shifts of the backscattered signal. To obtain two interferometric SAR (InSAR) images with a short time lag from a moving platform, one needs two antennas separated by a corresponding distance in flight direction. Accordingly, the technique is called along-track interferometry, not to be confused with cross-track interferometry (XTI) for topographic mapping. As mentioned above, the ATI concept was first proposed by Goldstein and Zebker (1987). First airborne ATI results were shown by Goldstein et al. (1989). Thompson and Jensen (1993) presented results of another experiment and demonstrated the importance of correcting ATI-derived velocity fields for contributions of wave motions. They were able to estimate required corrections theoretically. Further airborne ATI experiments were carried out, for example, by Ainsworth et al. (1995), Graber et al. (1996), Siegmund et al. (2004), Bjerklie et al. (2005), Romeiser (2005), and Toporkov et al. (2005).

The time lag τ between the two ATI images is determined by the along-track antenna separation L and platform velocity V. Depending on the transmit/receive sequence of the antennas, one obtains $\tau = L/V$ or $\tau = L/2\,V$, where L or $L/2$, respectively, is called effective baseline. For current measurements, τ needs to be sufficiently long to obtain significant phase signatures from current variations of interest and sufficiently short to avoid phase ambiguities and a decorrelation of the backscattered signal. The decorrelation time depends on radar frequency and wind/wave conditions. According to model results of Romeiser and Thompson (2000), decorrelation times at X band (10 GHz) and L band (1 GHz) are on the

order of 5–15 ms and 50–150 ms, respectively, where the lower (higher) values are for high (low) wind speeds. For a satellite ($V \approx 7$ km/s) this translates into maximal along-track antenna distances between about 35 and 2,100 m for different system parameters and wind conditions.

While temporal decorrelation at long time lags can lead to a useless quasi-uniform phase difference distribution with no recoverable velocity information, a low signal-to-instrument-noise ratio at short time lags can be reduced by averaging over a sufficient number of independent full-resolution pixel values, since the instrument-related phase noise is a zero-mean contribution. The number of phase samples that need to be averaged to obtain velocity estimates with a given accuracy is a good measure of the data quality of an ATI system, since it describes the relation between measuring accuracy and effective spatial resolution. Two diagrams showing the theoretical behaviour of this parameter as function of effective ATI baseline and instrument noise level for a spaceborne ATI system ($V = 7{,}000$ m/s) at X band, VV (vertical transmit and receive) polarisation, an incidence angle of 30°, and wind speeds of 5 and 15 m/s are shown in Fig. 5.1. Ideal baselines for the given parameters are in the range of about 20–40 m. Black dots indicate that the parameters of the X band section of the radar system used for the Shuttle Radar Topography Mission (SRTM) and of TerraSAR-X are clearly suboptimal. As will be shown later, the current fields obtained from these two systems have an effective spatial resolution on the order of 1 km, which is consistent with these diagrams.

ATI images are affected by the same velocity-related SAR mapping artefacts as conventional SAR images, and detected velocities need to be corrected for contributions of sub-resolution-scale wave motions, which may vary within an image due to wave-current interaction (Thompson and Jensen, 1993; Romeiser and Thompson, 2000). An iterative correction on the basis of numerical simulations was demonstrated by Romeiser (2005).

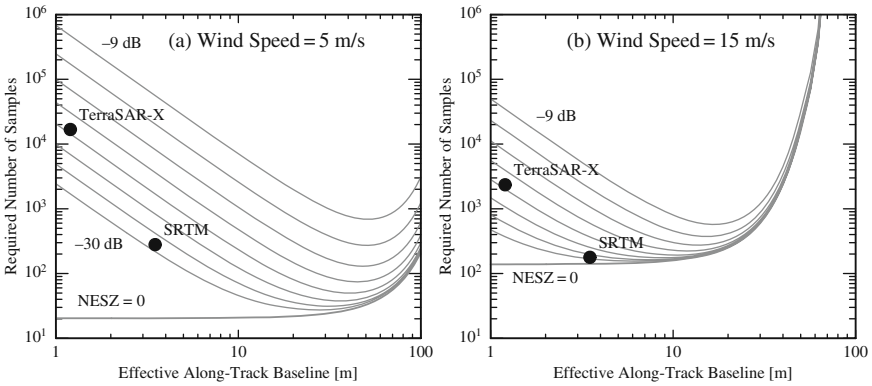

Fig. 5.1 Theoretical number of ATI phase samples to be averaged to obtain current estimates with an rms error of 0.1 m/s vs. effective along-track baseline, for instrument noise levels (NESZ) of 0 and −30 to −9 dB in steps of 3 dB and for wind speeds of 5 and 15 m/s. Radar frequency = 9.65 GHz, polarisation = VV, incidence angle = 30°. *Black dots* indicate properties of SRTM and TerraSAR-X

5.2.2 Doppler Centroid Anomaly Analysis

Direct instantaneous frequency determination from the phase history analysis of single antenna returns is a standard methodology to process SAR images (e.g. Madsen, 1989). Single-antenna Doppler estimates can indeed be directly obtained from the measured return signal spectral peak frequencies, i.e. Doppler centroids. Such estimates are commonly used to focus the SAR image. However, when compared to geometrically predicted Doppler frequencies (considering the relative motion between satellite and rotating earth), systematic differences or Doppler shift anomalies were reported for conventional SAR ocean scenes (Chapron et al., 2002). Analysis of global Wave Mode data from ENVISAT ASAR (one 10 km $\times$ 6 km "imagette" every 100 km) proved that these Doppler anomalies originated from geophysical conditions. Their analysis works best for homogeneous scenes, exhibiting small image intensity variations, and yields estimates with a spatial resolution of about 8 km $\times$ 4 km for ENVISAT ASAR Wide Swath Mode images (swath width $\approx$ 400 km) and 1 km $\times$ 1 km for ERS and ENVISAT Image Mode products (swath width $\approx$ 100 km). Note that the azimuthal resolution can be significantly better than the real aperture resolution of the radar antenna on the order of 5 km, since the Doppler centroid analysis can be combined with some amount of SAR processing. Like in ATI data processing, there is a tradeoff between the effective spatial resolution and the relative rms error (compared to the local expectation value) of retrieved radial velocity maps. From ASAR Wave Mode data, one velocity estimate is obtained every 100 km along the track.

As interpreted (Chapron et al., 2005; Johannessen et al., 2008), the Doppler anomaly is associated with an overall bulk velocity including the mean velocity of the radar detected surface scatters and the desired ocean surface current. The Doppler anomaly has been found to depend on radar frequency, incidence angle, polarisation, and environmental conditions, mostly wind speed and direction (Mouche et al., 2008). The mean velocity of the radar detected scatterers is generally larger for HH than VV polarisation and decreases with the radar wavelength and for incidence angles greater than 30°. Although no direct comparison has been performed so far, the physical mechanisms that lead to differences between actual surface currents and uncorrected Doppler velocities obtained from Doppler centroid anomalies seem to be the same as the ones that affect ATI data (Thompson and Jensen, 1993; Romeiser and Thompson, 2000; Romeiser, 2005).

The partitioning of the Doppler anomaly to the different contributions is a challenging problem, but the technique is robust and has the potential to meet high spatial resolution requisites. In all cases, the measurement of Doppler anomalies can complement the generation of conventional SAR images, so that geometrical and dynamical properties of the ocean scene can be derived together. Under favourable and well known environmental conditions, it is highly feasible to clearly identify mesoscale and submesoscale features and to infer absolute surface velocities along the radar line-of-sight direction, as pointed out by Johannessen et al. (2008).

5.3 Experimental Results

While the single-antenna Doppler anomaly analysis can be applied to thousands of existing SAR images from the last 2 decades, the archive of existing spaceborne ATI images of ocean scenes is limited to a few images from the 11-day SRTM mission in February 2000 and a few test images that have been acquired with TerraSAR-X since spring 2008. Here is a summary of key results we have obtained so far.

5.3.1 Along-Track InSAR Results

The single-pass XTI system installed on space shuttle *Endeavour* for the SRTM mission in February 2000 had an along-track antenna distance of 7 m (in addition to the cross-track distance of 60 m, which is not relevant for current measurements), which permitted current retrievals at a few test sites of opportunity, while the primary mission objective was topographic mapping over land (Rabus et al., 2003). TerraSAR-X, launched in June 2007, has a programmable phased-array antenna panel that can be divided into two parts with a theoretical phase center distance of 2.4 m for receiving. In both cases, the effective baseline is half the given distance, and the effective ATI time lags are clearly suboptimal (see Fig. 5.1), but the data have been good enough for a demonstration of current measurements from space by ATI. Figure 5.2 shows artistic views of SRTM and TerraSAR-X.

Figure 5.3a shows a line-of-sight current field retrieved from an interferometric X band image of the Dutch Wadden Sea from SRTM (from Romeiser et al., 2005). Due to the required pixel value averaging for noise reduction (see Fig. 5.1), the

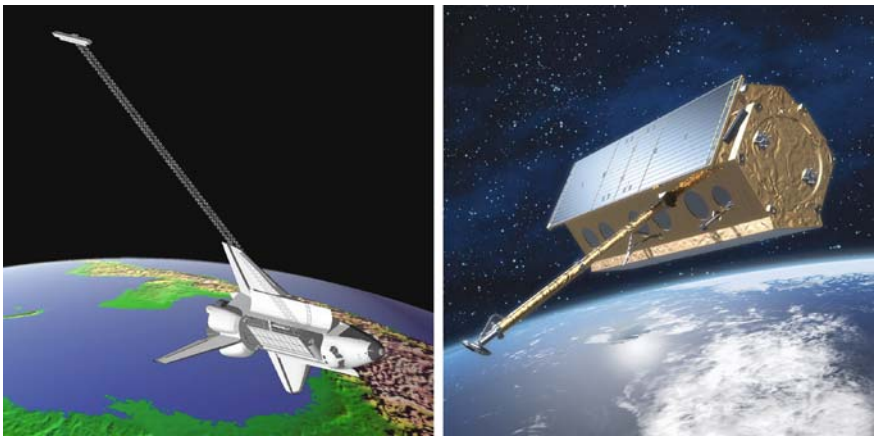

Fig. 5.2 Artistic illustrations of SRTM (*left*, courtesy NASA/JPL-Caltech) and TerraSAR-X (*right*, Siemens press picture) in space. The SAR antennas of SRTM are in the cargo bay and at the end of the 60-m long boom; the SAR antenna of TerraSAR-X is the *grey panel* at the *bottom*

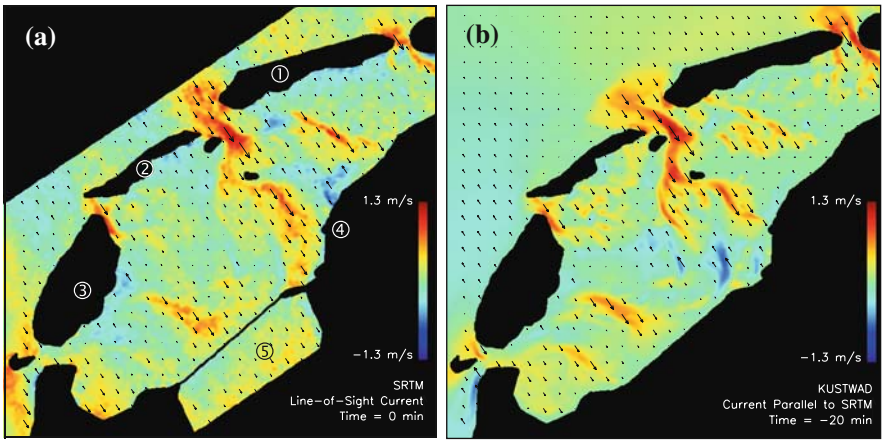

Fig. 5.3 Current field in the Dutch Wadden Sea from (**a**) SRTM and (**b**) a numerical circulation model. Area size = 70 km × 70 km, grid resolution = 100 m × 100 m. Map legend: 1 Terschelling, 2 Vlieland, 3 Texel, 4 Harlingen, 5 Lake IJssel

effective spatial resolution is on the order of 1 km, and the rms difference between SRTM-derived currents and reference currents from the numerical circulation model KUSTWAD (ten Cate et al., 2000) was found to be better than 0.1 m/s (Fig. 5.3b).

Romeiser et al. (2007) used another SRTM image to retrieve currents in the Elbe river (Germany). Results are shown in Fig. 5.4. Assuming that the dominant flow is

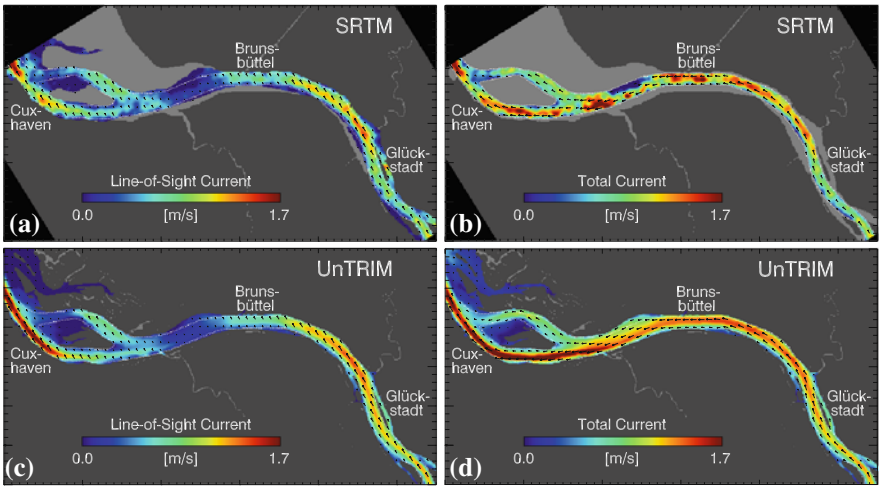

Fig. 5.4 Current field in the Elbe river (Germany); (**a**) SRTM-derived line-of-sight currents, (**b**) SRTM-derived quasi-2-D total surface currents, (**c**) model-derived component parallel to the look direction of SRTM, (**d**) model-derived total 2-D current field. Area size = 55 km × 30 km, grid resolution = 100 m × 100 m

parallel to the river bed, it was possible to construct a fully 2-D surface current field (Fig. 5.4b) from the ATI-derived component (Fig. 5.4a). Again, the SRTM-derived currents were found to be consistent with a numerical model or the river, UnTRIM (Casulli and Walters, 2000).

The divided antenna of TerraSAR-X has an even shorter ATI time lag than SRTM, and the instrument noise level is higher. However, according to Romeiser and Runge (2007), the smaller pixel size of TerraSAR-X permits more averaging of original pixel values at the same efffective spatial resolution (see also Fig. 5.1), which actually overcompensates the phase sensitivity and instrument noise handicap. The effective spatial resolution of current fields from TerraSAR-X in stripmap mode (swath width = 30 km, nominal pixel resolution = 3 m) was expected to be better than 1 km at an rms error of current estimates of 0.1 m/s. A major advantage of TerraSAR-X compared to SRTM is the pure ATI geometry of the divided antenna, which facilitates absolute current measurements. With a pure ATI system, a phase difference of 0 corresponds to a line-of sight velocity of 0, while phase differences from combined ATI/XTI systems include a topographic contribution that is often not well known.

ATI data acquisitions with TerraSAR-X are possible in various modes of operation, all of which are still in an experimental stage of development. In spring and summer 2008, a first series of ATI images was acquired in the so-called Aperture Switching (AS) mode, which uses a single receiver for both antenna halves in an alternating way at a doubled pulse repetition frequency. This is less desirable, but easier to implement than the full Dual Receive Antenna (DRA) mode, which uses two receivers in parallel. In AS mode, the swath width of stripmap images is reduced to about 16 km, the noise level is a little higher than in DRA mode, and ambiguities in the SAR processing can produce ghost images of bright targets on land over water. Nevertheless, Romeiser et al. (2010) were able to process and analyse six AS-mode images of the Elbe river quite successfully. Again, UnTRIM model results were used as reference. Example results for three of the six cases are shown in Fig. 5.5. The data quality of TerraSAR-X AS-mode data seems to be consistent with the theoretical predictions, and the retrieval of absolute currents from the pure ATI data of TerraSAR-X (in contrast to relative current variations within the scene from SRTM data) seems to work, but a final quantitative evaluation has not yet been done due to the preliminary state of the existing data processing routines.

5.3.2 Doppler Anomaly Analysis Results

At first order, the Doppler anomaly is mostly wind dependent, as revealed when collocated monthly wind fields from the European Centre for Medium Range Weather Forecasts (ECMWF) were projected along the radial direction of ENVISAT ASAR Wave Mode data. Based on the collocated data set obtained this way, a neural network model, called CDOP, was created for an incidence angles of 23° and 33°, where inputs are wind speed and relative wind direction with respect to azimuth;

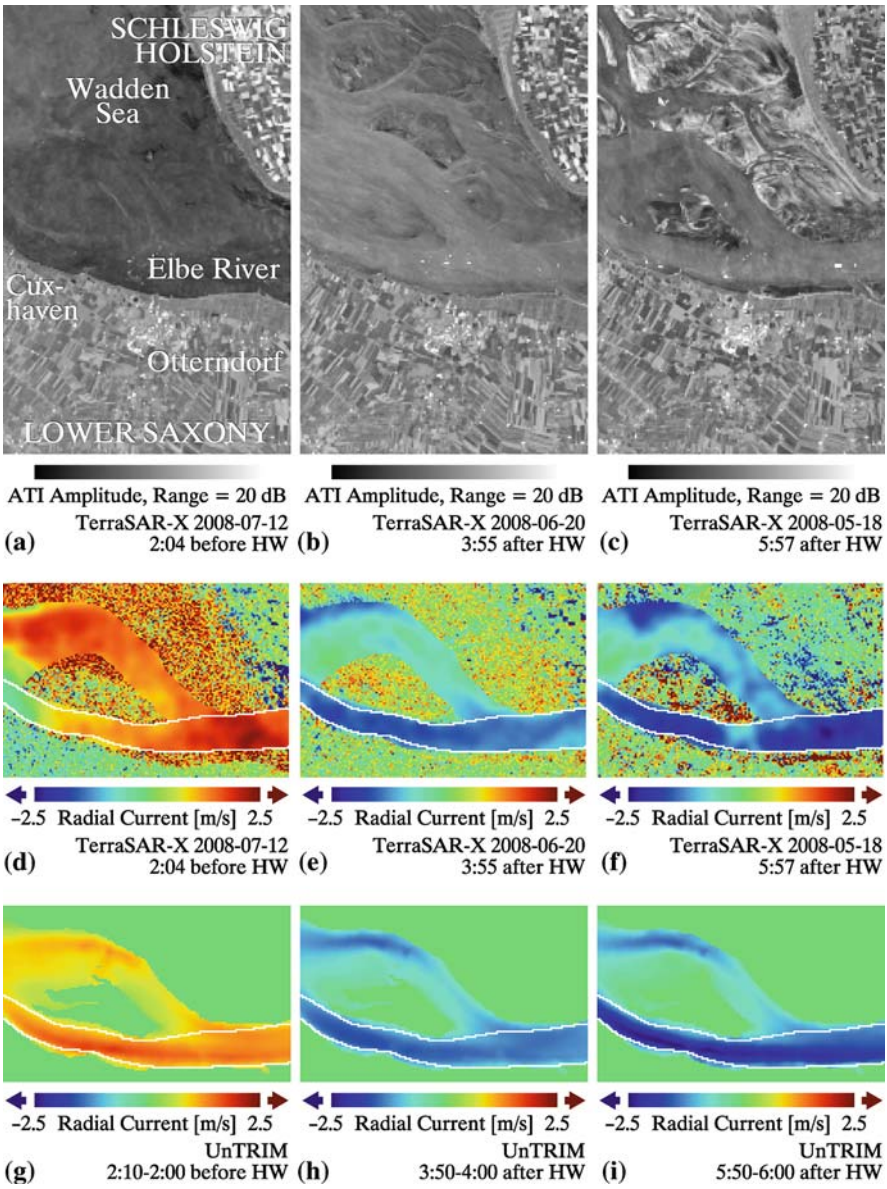

Fig. 5.5 First TerraSAR-X ATI results for the Elbe river; (**a**–**c**) three amplitude images acquired on different days at different tidal phases, (**d**–**f**) corresponding ATI-derived line-of-sight current fields, (**g**–**i**) corresponding line-of-sight current fields according to numerical model UnTRIM. Area size (amplitude images) = 16 km × 25 km, grid resolution = 100 m × 100 m, look direction = *left to right*, incidence angle = 31.0° (near range) to 32.5° (far range)

output is the wind-dependent contribution to Doppler velocities. Later, using the Doppler grid now available for each Wide Swath product, the CDOP model was extended to incidence angles from 17° to 42° (Collard et al., 2008).

Taking benefit of the large number of ASAR imagette observations and the development of CDOP, the detection capability of the Pacific equatorial current regime was examined. A monthly averaged residual radial current field, obtained after the removal of the wind effect, is presented in Fig. 5.6a. It exhibits a band with significant easterly (negative) directed radial velocities around 7°N latitude and two bands of westerly (positive directed) values on either sides centered at 2°N and 13°N latitude. This latitudinal variation of the line-of-sight surface current is in agreement with the expected positions of the equatorial current and counter current.

The zonal flow field at three selected transects was compared to zonal surface currents from the numerical global ocean circulation model MERCATOR (http://www.mercator-ocean.fr/), the drifter-derived climatology of global near-surface currents produced by the National Oceanic and Atmospheric Administration (NOAA) in the framework of the Global Drifter Program, and surface currents derived from altimetry data and wind field analysis from NOAA through the Ocean Surface Current Analyses – Real Time (OSCAR) project (Bonjean and Lagerloef, 2002). As shown in Fig. 5.6b–d, the overall agreement is noteworthy. The location of

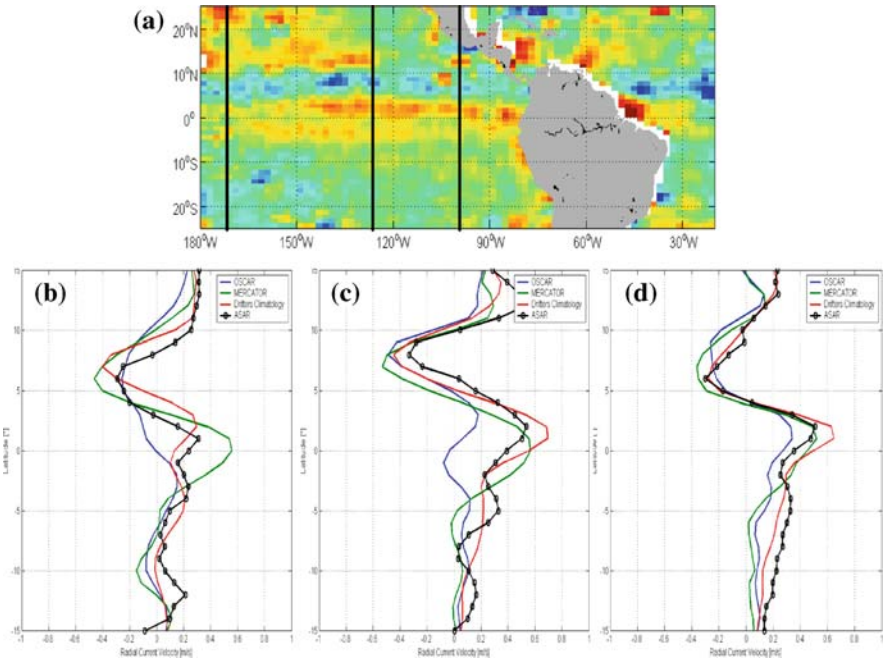

Fig. 5.6 Monthly mean residual radial surface velocity in November 2006 at 2° × 1° resolution from Doppler anomaly analysis (**a**) and comparison of radial velocities from MERCATOR, OSCAR, drifters, and ASAR at (**b**) 170°W, (**c**) 128°W, (**d**) 100°W and latitudes from 10°S to 10°N (*black lines* in (**a**))

the equatorial currents and counter currents are predicted and measured at the same latitudes, while the range of SAR-derived radial currents agrees with the surface current predictions and the independent measurements.

Using the ASAR wide swath mode, synoptic imaging of intense current regimes is also possible. After removal of the wind contribution to the Doppler signal over the Agulhas Current, it is evident that this residual surface velocity is connected with the strength and pathway of the greater Agulhas Current (Gründlingh, 1983), as demonstrated by Johannessen et al. (2008). Residual line-of-sight velocities reach 2 m/s in the Agulhas Current and nearly 1.5 m/s in the return current, as shown in Fig. 5.7. Currents of this magnitude were found to be consistent with

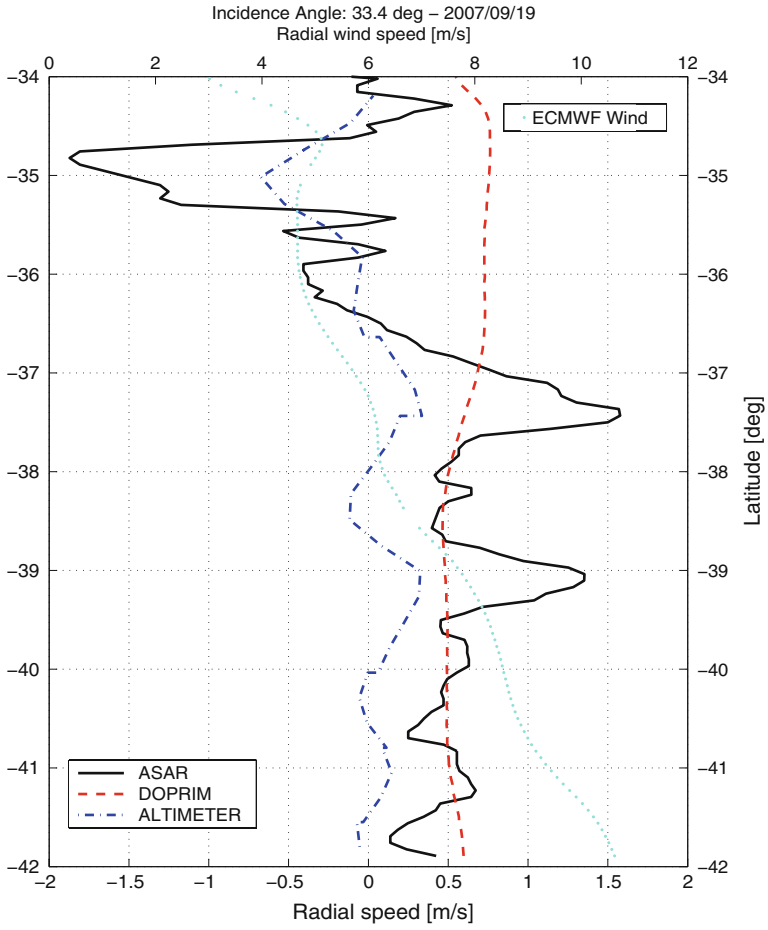

Fig. 5.7 Range-directed velocities along a transect in azimuth through the ASAR image of Fig. 5.8b: Residual velocity from Doppler anomaly analysis (*solid black*), geostrophic current according to altimeter data (*blue dash-dot*), wind-induced Doppler velocity contribution according to numerical model DopRIM (*red dashed*). *Light-blue dotted line* shows radial wind speeds from ECMWF

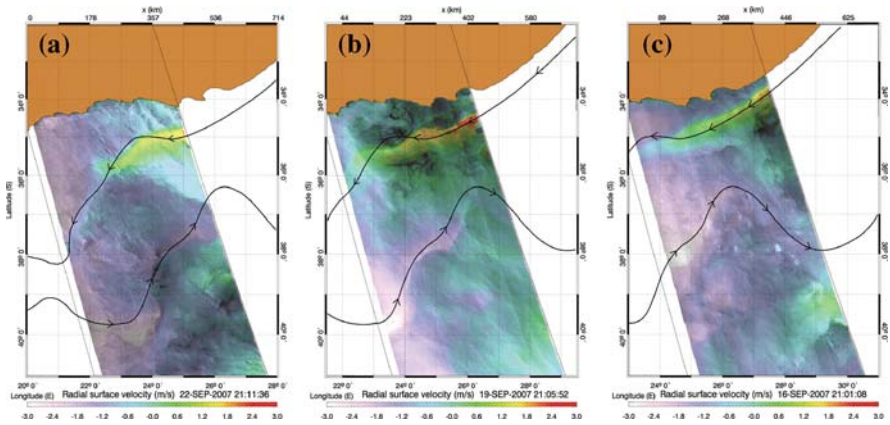

Fig. 5.8 Time series of range-directed Doppler velocity from ascending ASAR wide swath (420 km) images on (**a**) 22, (**b**) 19, (**c**) 16 September 2007 covering the greater Agulhas Current region. *Colour bar marks* radial velocities from −3 to +3 m/s. Positive speed is directed towards the SAR look direction (i.e. perpendicular to the swath, to the *left*). *Black curve* marks position of maximum geostrophic current derived from altimetry 7-day mean

drifter data, while altimeter data indicate a maximum geostrophic current of only about 0.7 m/s.

From this promising result, further evidence of the persistent range-directed surface velocity magnitude and pattern associated with the greater Agulhas Current can be assessed by the time series shown in Fig. 5.8 for acquisitions on 22, 19, and 16 September 2007. The full validation of such measurements remains a challenge as coincident direct sea surface current measurements are non-existent.

5.4 Outlook

Doppler centroid estimates are now included in ASAR image products from ESA. TerraSAR-X ATI acquisitions over selectable test areas should be available to registered users at the time of publication of this paper. Furthermore, a second TerraSAR-X type satellite called TanDEM-X (Moreira et al., 2004) should have been launched for formation flight with TerraSAR-X. While its main purpose is a high-resolution topographic mapping of land surfaces, the combination of TerraSAR-X and TanDEM-X will also enhance the ATI capabilities. In certain latitude bands, the along-track distance between the two satellites will permit ATI with a longer baseline and a corresponding improved accuracy and spatial resolution of surface current measurements. Furthermore, it may be possible to rotate TerraSAR-X and TanDEM-X into slightly different look directions and operate them both in split-antenna mode for two-dimensional vector current measurements, as proposed by Schulz-Stellenfleth et al. (2006; see also Frasier and Camps, 2001; Toporkov et al., 2005). ESA is currently considering the possibility to fly a passive bi-static SAR antenna in ATI formation with SENTINEL-1. On the long term, technically

optimised ATI satellites for ocean applications could permit vector current measurements at an effective spatial resolution of 100 m and with improved spatial and temporal sampling characteristics. The technology for such instruments is readily available. Further development in this field must be driven by user demand and should include dedicated validation campaigns. In the following we discuss promising applications. Some text and figures have been adapted from Romeiser and Runge (2008).

5.4.1 Global Oceanography

Chapron et al. (2005) have demonstrated the generation of global surface current maps at a spatial resolution on the order of 100 km from ENVISAT ASAR Wave Mode data. Johannessen et al. (2008) have shown that ASAR Wide Swath data can reveal large surface currents of the Agulhas Current that are not detected by altimeters.

Both capabilities can be very useful for global circulation studies as well as for studies on the dynamics of strong mesoscale current features in certain areas. The potential spatial resolution improvement of the ATI technique by more than one order of magnitude can be useful for studies on small-scale current features that have a strong larger-scale effect on the upper-ocean circulation as well as on chemical and biological processes.

For example, McGillicuddy et al. (2007) describe a stimulation of mid-ocean plankton blooms by eddy/wind interactions. Some of the eddies of interest can be seen in altimeter data, but an analysis of high-resolution current fields from single-antenna Doppler anomaly or ATI measurements, ideally in combination with water colour and temperature data from other sensors, would be highly desirable for more detailed investigations and improved model developments in this field.

5.4.2 Coastal Oceanography

The general circulation patterns in coastal seas are often well known and reproducible by numerical circulation models. Furthermore, many HF radars have been installed within the last decade for a continuous monitoring of currents, waves, and ship traffic in coastal regions (e.g. Gurgel and Schlick, 2007). However, quasi-geostrophic dynamic processes on spatial scales of 1–10 km are still not entirely understood, and they may be of interest for scientists and other users who are unable to install coast-based remote sensing systems or to perform extensive in-situ measurements. Such processes include the formation of mesoscale eddies, fronts, internal waves, the response of upper layer dynamics to rapid changes in the wind field, or effects of changes in bottom topography, river discharges, or other boundary conditions that are not well known and difficult to predict with purely theoretical approaches. Despite the coarse temporal sampling, repeated high-resolution current measurements from space can be valuable for basic research and routine monitoring in such regions.

5.4.3 Bathymetric Mapping and Monitoring

The mapping and monitoring of underwater bathymetry in coastal waters with strong tidal currents (for example, the Wadden Sea off the coast of the Netherlands, Germany, and Denmark) on the basis of conventional SAR intensity imagery was demonstrated by Calkoen et al. (2001) and has been available as an operational commercial service for several years. This technique exploits that bathymetric features become visible in SAR images due to a modulation of the tidal flow by the spatially varying water depth and a corresponding surface roughness modulation via wave-current interaction.

Since the imaging mechanism is quite indirect and includes several nonlinearities and dependencies on parameters that are not well known, the inversion is done through an iterative optimisation scheme for water depths and model parameters, which are modified until best possible agreement between observed and simulated radar image intensity variations is obtained with correct depths at known calibration points. This method is sufficient for the identification of major bathymetric changes, which can then be examined in more detail by conventional echosoundings. This way, the use of SAR data improves the cost efficiency of ship operations of the responsible monitoring agencies.

Even more improvement can be expected from the use of ATI data instead of conventional SAR images, since the relation between water depths and surface currents is clearly more direct than the one between water depths and SAR image intensities. Romeiser et al. (2002) demonstrated a bathymetric mapping on the basis of airborne ATI data using a very simple approach, exploiting just linearised surface current – water depth relations derived from reference data at a few locations in the test area by a regression analysis. An example result from an experiment at the German island of Sylt is shown in Fig. 5.9. In combination with a full physics-based flow model, such as the one used by Calkoen et al. (2001), bathymetry retrievals from ATI data should be more accurate and reliable than the conventional SAR-based approach, and the method should be applicable to more complex scenarios since the data interpretation is less ambiguous.

5.4.4 Coastal and Offshore Engineering

Coastal and offshore engineers are interested in effects of currents, waves, and winds on shore and water based structures, as well as effects of modifications of such structures. For example, British and German engineers have recently formulated requirements for the site selection of electric power generators in tidal waters and for further investigations on variations in the 3-D flow around such generators (European Commission, 2005). While it is obvious that the turbines should be placed in areas with long periods of strong and uniform currents, data from a British prototype system indicate that currents acting on the rotor exhibit unexpected strong variations on short time scales, which affect efficiency and wear of the device quite strongly. To study and optimise the relevant dynamic processes systematically,

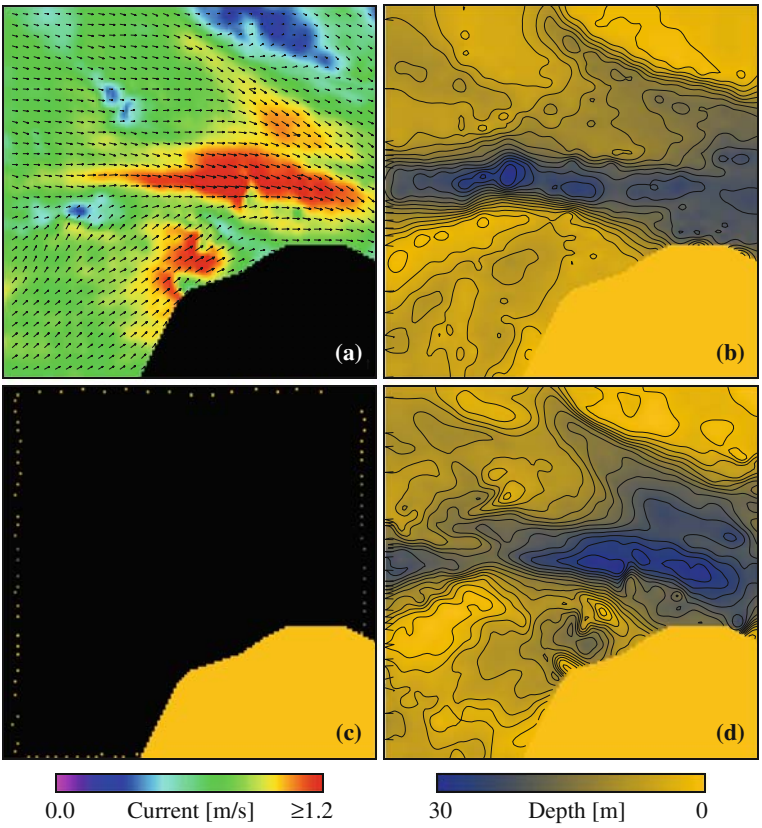

Fig. 5.9 Bathymetry retrieval example; (**a**) airborne ATI-derived current field north of the German island of Sylt; area size = 3.5 km × 3.5 km, grid resolution = 25 m × 25 m; (**b**) depth map from echosoundings with an effective resolution of 200 m; (**c**) 78 selected reference depth points near the boundaries; (**d**) depth map derived from the reference depths in combination with the ATI-derived current field

high-resolution and consistent wind, wave, and surface current measurements in combination with theoretical investigations are required. SAR/ATI-based measurements can make a significant contribution to this specific research as well as to similar offshore engineering tasks.

5.4.5 River Runoff Monitoring

Another promising field of application is the monitoring of river runoff, which is important for coastal oceanography, hydrology, and climate research. Furthermore, the redistribution of water due to climate changes and changes in population, industrialisation, and land use can have major effects on the earth system and on economical and political developments. At present, many rivers are monitored locally, and data from stations throughout the world are collected and archived at the Global

Runoff Data Centre (GRDC) in Koblenz, Germany. However, in some regions measurements are practically impossible for various reasons, and many countries do not publish existing runoff data. The development of a satellite-based monitoring system is highly desirable (Alsdorf et al., 2003).

British scientists have already demonstrated the monitoring of water levels in rivers on the basis of reprocessed conventional radar altimeter data (Berry, 2002). Concepts for more specific high-resolution altimeter missions for river applications has been proposed to ESA and NASA. The use of stationary microwave Doppler scatterometers for current measurements in rivers has been demonstrated by Plant et al. (2005).

Results of current retrievals in the Elbe river by SRTM and TerraSAR-X ATI have been discussed in Section 5.1. Scientists at the University of Hamburg are currently studying concepts for a data synthesis system for optimal river runoff assessments on the basis of spaceborne ATI and altimeter data, other available data, and numerical model computations.

An example of a velocity field in the Amazon river from ENVISAT ASAR, obtained using the Doppler anomaly technique, is shown in Fig. 5.10. The outflow direction is well aligned with the radar look direction. The surface velocity is quite

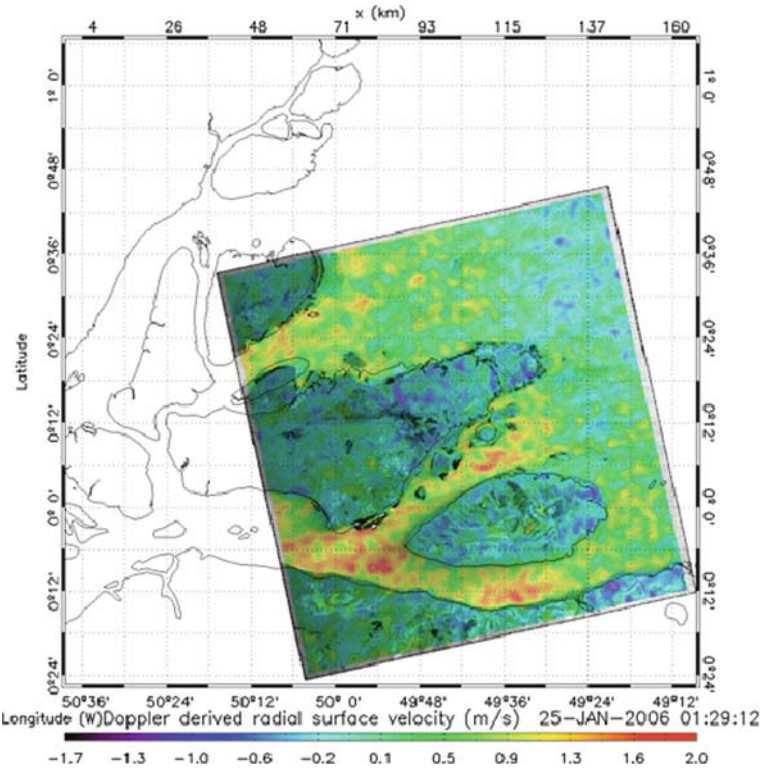

Fig. 5.10 Doppler velocity field in the Amazon river mouth, as obtained from ENVISAT ASAR data using the Doppler anomaly analysis technique

inhomogeneous and variable, as can be expected in the river mouth of this strong river, which possibly passes a range of different water depths that would trigger bands of acceleration and deceleration.

5.5 Summary and Conclusions

We have given an overview of the state of the art in the field of high-resolution surface current measurements from space by conventional and interferometric SAR, including a description of the two existing techniques, a review of experimental results from ENVISAT ASAR and TerraSAR-X, and a discussion of possible and desirable further developments and promising applications. While the basic concepts of Doppler anomaly analysis of conventional SAR data and of along-track interferometry were developed earlier, it was in the last decade that first successful current measurements from space by both methods could be demonstrated, using conventional SAR data from ERS and ENVISAT and interferometric SAR data from SRTM. With the development of robust data processing and correction methods, the addition of Doppler information to standard ASAR data products from ESA, and the implementation of experimental ATI capabilities on TerraSAR-X, conventional SAR- and ATI-based current measurements can now be made available for a variety of applications, and further development in this field will depend on user demand and financial support rather than on the solution of major technological problems.

The Doppler centroid anomaly analysis of conventional SAR data works with all SAR images (including archived ones) and provides maps of line-of-sight currents with spatial resolutions in the kilometer range within swaths of up to 400–500 km. The effective spatial resolution of ATI-derived line-of-sight current fields is on the order of 1 km within a swath of up to 100 km, but it could be improved by about one order of magnitude with improved system parameters (longer along-track baseline, reduced instrument noise) on future satellites. Furthermore, a spaceborne dual-beam along-track InSAR could measure two current components during a single overpass to obtain fully two-dimensional vector current maps.

So far we have demonstrated the retrieval of coarse-resolution global current maps from ENVISAT ASAR Wave Mode data and the observation of regional current features, such as the Agulhas Current, with Image Mode and Wide Swath data, as well as the imaging of current fields in coastal waters and rivers with ATI data from SRTM and TerraSAR-X. We see a variety of promising applications in the open ocean, coastal waters, and river estuaries, such as scientific studies on turbulence structures, shallow-water bathymetry monitoring, studies related to coastal and offshore engineering projects, and river runoff monitoring. Altogether, current measurements by spaceborne SAR and ATI seem to have the potential to become a widely used remote sensing technique, with a level of maturity comparable to radar altimetry, wind scatterometry, and SAR-based oil spill detection or wave spectra retrievals, within the coming 10 years.

Acknowledgements We thank H. Breit, M. Eineder, and U. Steinbrecher (DLR, Oberpfaffenhofen, Germany), M. Gade, S. Grünler, and J. Sprenger (University of Hamburg, Germany), N. Winkel, A. Sohrmann, and H. Weilbeer (BAW, Hamburg), W. Sent (BSH, Hamburg), and K. de Jong and J. Vogelzang (RWS, Netherlands) for important contributions to the research presented in this chapter. This work has been partly funded by the U.S. Office of Naval Research under grant N00014-09-1-0366.

References

Ainsworth TL, Chubb SR, Fusina RA, Goldstein RM, Jansen RW, Lee JS, Valenzuela GR (1995) INSAR imagery of surface currents, wave fields, and fronts. IEEE Trans Geosci Rem Sens 33:1117–1123

Alsdorf D, Lettenmaier D, Vörösmarty C, NASA Surface Water Working Group (2003) The need for global, satellite-based observations of terrestrial surface waters. EOS Trans AGU, 84(269):275–276

Berry PAM (2002) A new technique for global river and lake height monitoring using satellite altimeter data. Int J Hydropower Dams 9(6):52–54

Bjerklie DM, Moller D, Smith LC, Dingman SL (2005) Estimating discharge in rivers using remotely sensed hydraulic information. J Hydrol 309:191–209

Bonjean F, Lagerloef GSE (2002) Diagnostic model and analysis of the surface currents in the tropical Pacific Ocean. J Phys Oceanogr 32:2938–2954

Calkoen CJ, Hesselmans GHFM, Wensink GJ, Vogelzang J (2001) The bathymetry assessment system: efficient depth mapping in shallow seas using radar images. Int J Rem Sens 22: 2973–2998

Casulli V, Walters RA (2000) An unstructured grid, three-dimensional model based on the shallow water equations. Int J Numer Methods Fluids 32:331–348

Chapron B, Collard F, Ardhuin F (2005) Direct measurements of ocean surface velocity from space: interpretation and validation. J Geophys Res 110:C07008, doi:10.1029/2004JC002809, 17pp

Chapron B et al. (2002) Ocean geophysical results from ASAR. Presentation at ASAR Validation Review 2002, available at http://envisat.esa.int/workshops/validation_12_02/asar/wv-asar-validation-review_bchapron_12-dec-2002.ppt

Collard F, Mouche A, Chapron B, Danilo C, Johannessen JA (2008) Routine high resolution observation of selected major surface currents from space. Proceedings of the SeaSAR 2008, ESA Communication Production Office, ESTEC, Noordwijk, Netherlands, 8pp

Essen HH, Gurgel KW, Schlick T (2000) On the accuracy of current measurements by means of HF radar. IEEE J Oceanic Eng 25:472–480

European Commission (2005) SEAFLOW pilot project for the exploitation of marine currents. Final Report JOR3-CT98-0202, European Commission, Brussels

Frasier SJ, Camps AJ (2001) Dual-beam interferometry for ocean surface current vector mapping. IEEE Trans Geosci Rem Sens 39:401–414

Fu LL, Holt B (1982) Seasat Views Oceans and Sea Ice with Synthetic-Aperture Radar, JPL Publisher, Jet Propulsion Lab, Pasadena, CA, USA, pp. 81–120, 200

Goldstein RM, Barnett TP, Zebker HA (1989) Remote sensing of ocean currents. Science 246:1282–1285

Goldstein RM, Zebker HA (1987) Interferometric radar measurement of ocean surface currents. Nature 328:707–709

Graber HC, Thompson DR, Carande RE (1996) Ocean surface features and currents measured with synthetic aperture radar interferometry and HF radar. J Geophys Res 101:25813–25832

Gründlingh ML (1983) On the course of the Agulhas Current. S Afr Geogr J 65:49–57

Gurgel KW, Schlick T (2007) Land-based over-the-horizon radar techniques for monitoring the NE Atlantic coastal zone. In: Barale V, Gade M (eds.) Remote Sensing of the

European Seas, Springer Science and Business Media, Berlin, Heidelberg, New York, pp. 447–460

Johannessen JA, Chapron B, Collard F, Kudryavtsev K, Mouche A, Akimov D, Dagestad KF (2008) Direct ocean surface velocity measurements from space: improved quantitative interpretation of Envisat ASAR observations. Geophys Res Lett 35:L22608, doi:10.1029/2008GL035709, 6pp

Madsen SN (1989) Estimating the doppler centroid of SAR data. IEEE Trans Aerosp Electron Syst AES 25:134–140

McGillicuddy DJ et al. (2007) Eddy/wind interactions stimulate extraordinary mid-ocean plankton blooms. Science 316:1021–1026

Moreira A, Krieger G, Hajnsek I, Hounam D, Werner M, Riegger S, Settelmeyer E (2004) TanDEM-X: a TerraSAR-X add-on satellite for single-pass SAR interferometry. Proceedings of the IGARSS 2004, IEEE, Piscataway, NJ, 4pp

Mouche AA, Chapron B, Reul N, Collard F (2008) Predicted doppler shifts induced by ocean surface wave displacements using asymptotic electromagnetic wave scattering theories. Waves Random Complex Media 18:185–196

Palmer AJ (1991) Surface current mapping performance of bistatic and monostatic Δk-radars. IEEE Trans Geosci Rem Sens 29:1014–1016

Plant WJ, Keller WC, Hayes K, Spicer K (2005) Streamflow properties from time series of surface velocity and stage. J Hydr Eng 131:657–664

Rabus B, Eineder M, Roth A, Bamler R (2003) The shuttle radar topography mission – a new class of digital elevation models acquired by spaceborne radar. ISPRS J Photogramm Rem Sens 57:241–262

Romeiser R (2005) Current measurements by airborne along-track InSAR: measuring technique and experimental results. IEEE J Ocean Eng 30:552–569

Romeiser R, Breit H, Eineder M, Runge H, Flament P, de Jong K, Vogelzang J (2005) Current measurements by SAR along-track interferometry from a space shuttle. IEEE Trans Geosci Rem Sens 43:2315–2324

Romeiser R, Runge H (2007) Detailed analysis of ocean current measuring capabilities of TerraSAR-X in several possible along-track InSAR modes on the basis of numerical simulations. IEEE Trans Geosci Rem Sens 45:21–35

Romeiser R, Runge H (2008) Current measurements in coastal waters and rivers by along-track InSAR. In: Barale V, Gade M (eds.) Remote Sensing of the European Seas, Springer Science and Business Media, Berlin, Heidelberg, New York, pp. 411–422

Romeiser R, Runge H, Suchandt S, Sprenger J, Weilbeer H, Sohrmann A, Stammer D (2007) Current measurements in rivers by spaceborne along-track InSAR. IEEE Trans Geosci Rem Sens 45:4019–4030

Romeiser R, Seibt-Winckler A, Heineke M, Eppel D (2002) Validation of current and bathymetry measurements in the German Bight by airborne along-track interferometric SAR. Proceedings of the IGARSS 2002, IEEE, Piscataway, NJ, 3pp

Romeiser R, Suchandt S, Runge H, Steinbrecher U, Grünler S (2010) First analysis of TerraSAR-X along-track InSAR-derived current fields. IEEE Trans Geosci Rem Sens 48:820–829

Romeiser R, Thompson DR (2000) Numerical study on the along-track interferometric radar imaging mechanism of oceanic surface currents. IEEE Trans Geosci Rem Sens 38-II:446–458

Schulz-Stellenfleth J, Hajnsek I, Lehner S (2006) Use of TanDEM-X in a squinted split antenna mode configuration to retrieve 2-D current and ocean wave information. Proceedings of the IGARSS 2006, IEEE, Piscataway, NJ, USA, 4pp

Shuchman R (1979) The feasibility of measurement of ocean current detection using SAR data. Proceedings of the 13th International Symposium on Remote Sensing of Environment, Ann Arbor, MI, USA, pp. 93–103

Siegmund R, Bao M, Lehner S, Mayerle R (2004) First demonstration of surface currents imaged by hybrid along- and cross-track interferometric SAR. IEEE Trans Geosci Rem Sens 42: 511–519

ten Cate HH, Hummel S, Roest MRT (2000) An open model system for 2d/3d hydrodynamic simulations. Proceedings of the Hydroinformatics 2000, Int Assoc Hydraulic Engineering and Research, Madrid, Spain

Thompson DR, Jensen JR (1993) Synthetic aperture radar interferometry applied to ship-generated waves in the 1989 Loch Linnhe experiment. J Geophys Res 98:10259–10269

Toporkov JV, Perkovic D, Farquharson G, Sletten MA, Frasier SJ (2005) Sea surface velocity vector retrieval using dual-beam interferometry: first demonstration. IEEE Trans Geosci Rem Sens 43:2494–2502

Wunsch C, Stammer D (1998) Satellite altimetry, the marine geoid, and the oceanic general circulation. Ann Rev Earth Planet Sci 26:129–253